

Signatures of Nonergodicity in Sparse Random Matrices

Sagnik Seth,^{1,*} Adway Kumar Das,^{2,†} and Anandamohan Ghosh^{1,‡}

¹*Department of Physical Sciences, Indian Institute of Science Education and Research Kolkata, Mohanpur 741246, India*

²*School of Science, Loughborough University, Loughborough, Leicestershire LE11 3TU, United Kingdom*

The prevalence of sparsity in interacting many-body systems motivates an investigation into the spectral statistics of sparse random matrices with on-site disorder. We numerically demonstrate that the Anderson transition can be identified through the statistical properties of the ground state. By analytically deriving the energy moments and calculating the shifted kurtosis, we estimate the critical sparsity threshold for this localization-delocalization transition. The short-range energy correlation in the bulk indicates that the Anderson transition at infinite temperature coincides with the quantum phase transition. Furthermore, long-range energy correlations in the bulk spectrum reveal a Thouless energy scale, suggesting a broad nonergodic regime within the delocalized phase.

I. INTRODUCTION

Recent experimental advances in cold atoms [1], ion traps [2], superconducting qubits [3], nuclear magnetic resonance [4] have provided a fresh impetus to explore interacting many-body systems. In the presence of impurities, ergodicity often breaks down and a many-body localized (MBL) phase is observed in the bulk energy spectrum [5–12]. Such an ergodic-MBL phase transition is reflected in the statistical properties of a sparse matrix representation of a many-body Hamiltonian which is analogous to a single-particle tight-binding model on a graph [13–15]. In Fig. 1, we show the Fock space graph for prototypical many-body systems like the Heisenberg and transverse field Ising models. Such hierarchical tree-like structures motivated studies on random regular graphs with on-site disorder which exhibit various interesting phenomena, e.g. Anderson delocalization-localization transition, breaking of ergodicity, sub-diffusive transport and violation of thermalization [16–18].

A typical signature of a MBL state is multifractality over the Fock space [19, 20]. Thus, it is imperative to study non-regular graphs as opposed to random regular graphs where multifractality is absent [21–23]. A prominent example of non-regular graph is the Erdős-Rényi-Gilbert graph, whose adjacency matrix is shown in Fig. 1(d) for the number of nodes $N = 64$ and the probability of finding a nonzero edge $p = 0.1$ [24, 25].

For Erdős-Rényi-Gilbert graph, there is a critical percolation limit $p = N^{-1}$ below which the graph is fragmented and above which there exists a giant connected component with a heterogeneous locally tree-like structure leading to a mobility edge separating localized and extended states in the energy spectrum [26]. Furthermore, random weights can be assigned to graph edges to generate a sparse or dilute random matrix model [27, 28] important for understanding various systems like dilute

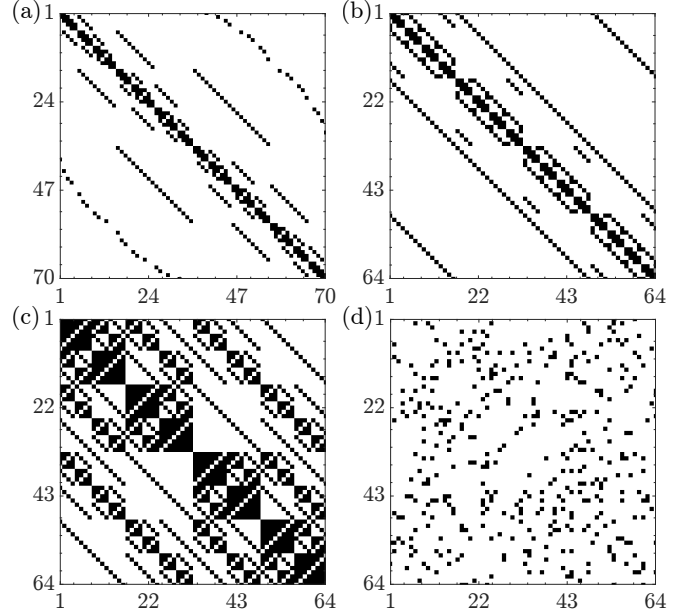


FIG. 1. **Matrix representations of various sparse Hamiltonians:** (a) 1D Heisenberg model with nearest neighbor interactions and periodic boundary condition in the zero magnetization sector for 8 spin- $\frac{1}{2}$ particles in the $\hat{\sigma}^z$ basis [32]. (b) Anderson model on $4 \times 4 \times 4$ cubic lattice with nearest neighbor hopping and periodic boundary condition in the site basis [33]. (c) Transverse field Ising model with long-range interaction in the odd-parity sector for 7 spin- $\frac{1}{2}$ particles in the $\hat{\sigma}^z$ basis [32]. (d) Adjacency matrix of an Erdős-Rényi-Gilbert graph on 64 nodes where the probability of finding a non-zero edge is 0.1 [25].

magnets [29], mean-field theory of spin glass [30, 31].

The spectral properties of the sparse random matrices have drawn considerable interests over the last three decades. The density of states (DOS) of a quantum system can be obtained from the Laplace transform of the complex partition function, which has been studied using the replica method in case of the sparse matrices [29, 34–38]. For $p \rightarrow 1$, the DOS follows the Wigner’s semicircle law while a tail is observed for $p < 1$ and finite N [28, 39, 40]. For $p > N^{-1}$, the spectral prop-

* ss22ms026@iiserkol.ac.in

† A.K.Das@lboro.ac.uk

‡ anandamohan@iiserkol.ac.in

erties of the giant connected component with random hopping terms and no self-loop is systematically studied in Ref. [27]. The absence of self-loop leads to extensively many degenerate eigenstates at zero energy, which are localized on the leaves of the connected component, leading to a divergence in the bulk DOS [41].

A power-law tail in the local density of states (LDOS) indicates a weak multifractality of the bulk states at non-zero energy where the fractal dimension D_1 is unity, i.e. the support set of the eigenstate intensities spans a finite fraction of all the nodes but $D_q < 1$ is q -dependent for some $q > q_*$, i.e. a vanishingly small number of nodes support anomalously large eigenstate intensities [42, 43]. In contrast, Anderson localized states exist at low energies which are separated from the multifractal extended states by a mobility edge [44–46].

The heterogeneous spectral properties of the weighted adjacency matrix are manifested in the non-equilibrium dynamics on Erdős-Rényi-Gilbert graphs. Particularly, the survival probability of an initially localized state exhibits a power-law decay at intermediate timescales dictated by the fractal dimension of the bulk energy states [27] and a metal-insulator transition is reflected in the scattering matrix elements [47].

In this work, we perturb the weighted adjacency matrix of the Erdős-Rényi-Gilbert graph by an on-site disorder and the resulting random matrices belong to the sparse Gaussian orthogonal ensemble (sGOE). Such a construction is motivated by the realistic disordered many-body systems, where the presence of impurities leads to diagonal disorder in the matrix representation. While the diagonal disorder lifts the degeneracy of the zero modes present in the adjacency matrix of the Erdős-Rényi-Gilbert graph, we find that the Anderson delocalization-localization transition still occurs at the critical percolation limit $p = N^{-1}$ and signatures of the transition are present in the ground states.

We numerically obtain the ground state using the wall-Chebyshev projector and look at the corresponding statistical properties. We find that the distribution of the ground state energy is well described by the Gumbel distribution for $p < N^{-1}$ whereas the Tracy-Widom distribution is valid only at the GOE limit ($p = 1$). The system size scaling of the moments of the ground state intensities as well as the bipartite entanglement entropy indicate that the ground state is localized for $p < N^{-1}$ but becomes a nonergodic extended state for $N^{-1} < p < 1$. Thus, sGOE exhibits a quantum phase transition at $p = N^{-1}$.

We analytically compute the energy moments of sGOE and find that the DOS has a transition from the Wigner’s semicircle law to Gaussian distribution at $p = N^{-1}$. Later we look at the energy correlations in the bulk spectrum and find that the short-range correlation is present for $p > N^{-1}$ and absent for $p < N^{-1}$. In the delocalized regime ($p > N^{-1}$), we identify the mobility edge by looking at the ratio of level spacing as a function of energy.

The measures of long-range energy correlations, e.g. the number variance and the power-spectrum of noise indicate the presence of a Thouless energy scale. Thus, away from the GOE limit and below the Anderson transition point, we find a nonergodic regime where a localized excitation may take a long time period (inversely proportional to the Thouless energy) to spread over the system compared to a typical ergodic system.

The organization of this paper is as follows: in Sec. II, we introduce the matrix model and its density in the matrix space. In Sec. III, we look at the density of the ground state energy, corresponding fractal dimensions and the entanglement entropy. In Sec. IV, we show the energy moments and the DOS. In Sec. V, we show the short- and long-range energy correlations while identifying the mobility edge and Thouless energy scale. Our concluding remarks are given in Sec. VI.

II. MODEL

Consider $\mathcal{A}(N, p)$, the adjacency matrix of the Erdős-Rényi-Gilbert graph with N number of nodes where $\mathcal{A}_{ii} = 0$ (i.e. no self-loop) and $\mathcal{A}_{ij} = \mathcal{A}_{ji}$ follows the Bernoulli distribution with a success rate p . If we define $p \equiv \frac{b \ln N}{N}$, $\mathcal{A}' \equiv \frac{\mathcal{A}}{\sqrt{b \ln N}}$ and exclude the Perron-Frobenius (largest) eigenvalue of \mathcal{A} , the energy spectrum of \mathcal{A}' is within ± 2 for $b > b_* \equiv (\ln 4 - 1)^{-1}$ [48] and all the energy eigenstates are ergodic [49–51]. For $b < b_*$, mobility edges exist at $E_* = \pm 2$, separating ergodic states at high energy from the nonergodic extended (NEE) states at low energy [26].

For a NEE state of \mathcal{A}' , there are extensive but vanishing fraction of resonant nodes, around which the eigenstate profile has exponential decay within disjoint balls. Corresponding eigenvalues are given by the nodes with abnormally large degree $\geq 2b \ln N$ [52]. The system size scaling of the maximum intensity of the energy states shows a sharp discontinuity across the mobility edges. Above properties remain valid for $\frac{\sqrt{\ln N}}{N} \ll p \ll \frac{\ln N}{N}$ whereas localized energy states appear corresponding to the leaves at the periphery of the graph for $p < \frac{\sqrt{\ln N}}{N}$.

We are interested in the spectral properties of the weighted adjacency matrices of sparse graphs. So, we look at the sparse Gaussian orthogonal ensemble (sGOE) consisting of $N \times N$ real symmetric random matrices H with sparsity $0 \leq p \leq 1$

$$H = H^{\text{Poisson}} + H^{\text{GOE}} \odot \mathcal{A}(N, p) \quad (1)$$

where H^{Poisson} is a diagonal matrix from the Poisson ensemble such that $H_{ii}^{\text{Poisson}} \sim \mathcal{N}(0, 1)$, H^{GOE} belongs to the Gaussian Orthogonal Ensemble (GOE) such that $H_{ij}^{\text{GOE}} \sim \mathcal{N}\left(0, \frac{1 + \delta_{ij}}{2}\right)$, $\mathcal{N}(\bar{x}, \sigma^2)$ is the Gaussian distribution with mean \bar{x} and variance σ^2 and $A \odot B$ implies the Hadamard product of two matrices A and B . On

average, H has $p\binom{N}{2} \sim \mathcal{O}(pN^2)$ off-diagonal elements. Consequently, for $p = 1$ ($p = 0$), we obtain a random matrix from GOE (Poisson ensemble). In Eq. (1), H^{Poisson} indicates the presence of on-site disorder and lifts the degeneracy at zero energy observed in the weighted adjacency matrix of the Erdős-Rényi-Gilbert graph [27].

Equation (1) implies that the elements of H have the following distribution

$$P(H_{ij}) = \begin{cases} \frac{1}{\sqrt{2\pi}} e^{-\frac{H_{ii}^2}{2}}, & i = j \\ (1-p)\delta(H_{ij}) + \frac{p}{\sqrt{\pi}} e^{-H_{ij}^2}, & i \neq j \end{cases} \quad (2)$$

The matrix elements, H_{ij} 's are independent up to symmetry, leading to a probability density in the matrix space

$$\begin{aligned} P(H) &= \prod_{i=1}^N P(H_{ii}) \prod_{i<j}^N P(H_{ij}) \\ &= \frac{(1-p)^{\frac{N(N-1)}{2}}}{(2\pi)^{\frac{N}{2}}} e^{-\frac{1}{2} \sum_{i=1}^N H_{ii}^2} \prod_{i<j}^N \left[\delta(H_{ij}) + \frac{pe^{-H_{ij}^2}}{(1-p)\sqrt{\pi}} \right] \end{aligned} \quad (3)$$

We want to interpolate between the GOE and Poisson limit by varying the sparsity of sGOE and study corresponding statistical properties. As the critical percolation limit is $p = N^{-1}$, a convenient reparameterization of the sparsity is

$$p \equiv N^{-\frac{\gamma}{2}} \quad (4)$$

such that $\gamma = 0$ ($\gamma \rightarrow \infty$) is the GOE (Poisson) limit. As the critical percolation limit of Erdős-Rényi-Gilbert graph is $p = N^{-1}$, $\gamma = 2$ should be the critical point where delocalization-localization transition occurs, which we establish later via energy correlations.

III. GROUND STATE

In case of the Poisson ensemble, the energy levels follow the Gaussian distribution with a tail decaying faster than the power-law while the domain is unbounded. Consequently, the ground state of the Poisson ensemble follows the reflected Gumbel distribution [53]

$$P_{E_1}(y) = \frac{1}{\eta_N} \exp\left(\frac{y + \mu_N}{\eta_N} - \exp\left(\frac{y + \mu_N}{\eta_N}\right)\right). \quad (5)$$

where the location (μ_N) and scale (η_N) parameters are [54]

$$\mu_N = g\left(1 - \frac{1}{N}\right), \quad \eta_N = g\left(1 - \frac{1}{Ne}\right) - \mu_N \quad (6)$$

where $g(x) = \sqrt{2}\sigma_E \text{erf}^{-1}(2x - 1)$ is the inverse of the cumulative distribution of energy for the Poisson ensemble.

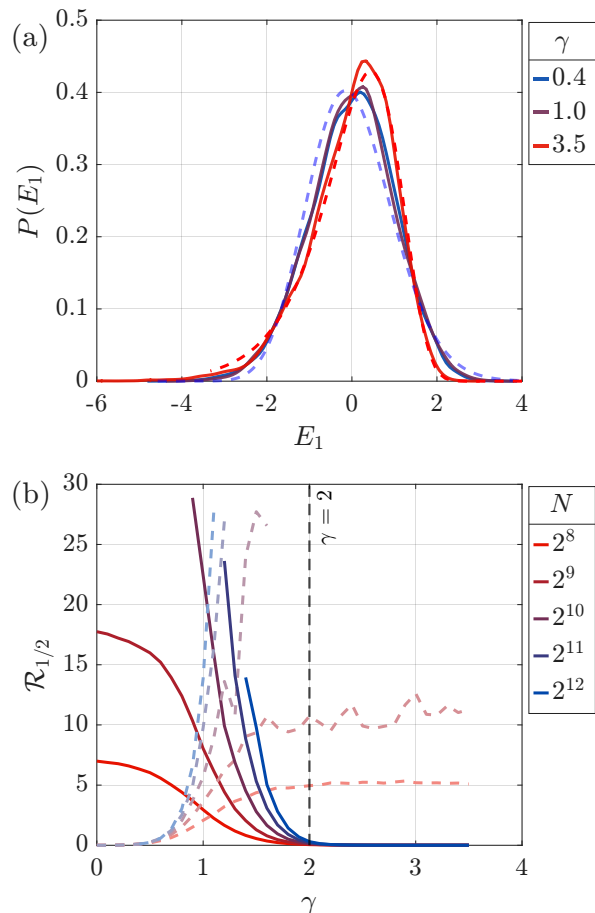


FIG. 2. **Ground state energies of sGOE.** (a) density of the ground state energies obtained using the wall-Chebyshev projector [55] for $N = 16384$ and different values of γ . The energy levels are shifted and scaled to ensure zero mean and unit variance. Dashed red (blue) curve denotes the Gumbel (Tracy-Widom) distribution. (b) Rényi divergence of order $q = \frac{1}{2}$ between the numerical histogram of the ground state and the Gumbel (Tracy-Widom) distribution as a function of γ for different system sizes shown via solid (dashed) lines.

In the case of Wigner-Dyson ensembles, the extreme eigenvalues follow the Tracy-Widom distributions [56–58]. The average ground state energy for the GOE is [59]

$$\begin{aligned} \langle E_1 \rangle &= -\frac{\sigma_E}{\sqrt{\frac{N+1}{2}}} \left(\mu_N + \eta_N E_{\text{TW}}^{(1)} \right) \\ \mu_N^2 &= 2 \left(N - \frac{1}{2} - \frac{(N - \frac{1}{2})^{-\frac{1}{3}}}{10} \right), \quad \eta_N = \frac{N^{-\frac{1}{6}}}{\sqrt{2}} \end{aligned} \quad (7)$$

where $E_{\text{TW}}^{(1)} = -1.20653357458\dots$ is the expectation value w.r.t. Tracy-Widom distribution with unit Dyson index.

In the case of sGOE, we expect the Gumbel distribution to be valid in the limit $p \rightarrow 0$ and Tracy-Widom for $p \rightarrow 1$. To study the distribution of the lowest energy of sGOE for intermediate values of p , we obtain the corre-

sponding ground state using the wall-Chebyshev projector [55]. Such an algorithm is based on the fact that the wall function

$$\text{wall}(x) = \begin{cases} \infty, & x < 0 \\ 1, & x = 0 \\ 0, & x > 0 \end{cases} \quad (8)$$

can be expanded in terms of the Chebyshev polynomials and $\text{wall}(H)$ applied to a random vector converges to the ground state of the Hamiltonian H . In Fig. 2(a), we show the density of ground state energy for different values of γ . To understand the validity of the Gumbel or Tracy-Widom distribution at different values of the sparsity parameter, we compute the Rényi divergence of order q [60]

$$\mathcal{R}_q = \frac{1}{q-1} \ln \left(\int dx (P(x))^q (P_{\text{test}}(x))^{1-q} \right) \quad (9)$$

where $P(x)$ is the numerically obtained histogram of the ground state energy and $P_{\text{test}}(x)$ is either Gumbel or Tracy-Widom distribution. In Fig. 2(b), we show the Rényi divergences as a function of γ for different system sizes. Our analyses show that if the test function is Gumbel distribution, the Rényi divergence increases (decreases) with system size for $\gamma < 2$ ($\gamma > 2$), i.e. the ground state energy of sGOE follows the Gumbel distribution for $\gamma > 2$, provided $N \gg 1$. This is expected as $\gamma = 2$ is the Anderson delocalization-localization transition point, beyond which the energy states are localized with uncorrelated energy levels. On the other hand, the Rényi divergence w.r.t. Tracy-Widom distribution is zero only at GOE limit, $\gamma = 0$, and increases with N for $\gamma > 0$.

Structure of ground state

The structure of the ground state, in particular the localization length and the fluctuations of the ground state intensities determine the nature of dynamics at low-temperature for a closed quantum system. To understand the localization properties of the ground state over the Hilbert space, we look at the generalized inverse participation ratios (IPRs) [61–65]

$$I_q^{(N)} = \sum_{n=1}^N |\Psi(n)|^{2q} \sim N^{(1-q)D_q^{(N)}} \quad (10)$$

where $\Psi(n) = \langle \Phi_n | \Psi \rangle$ is the n th component of the state vector $|\Psi\rangle$ in a chosen basis $\{|\Phi_n\rangle\}$, N is the Hilbert space dimension and $D_q^{(N)}$ is the q th finite size fractal dimension. By extrapolating $D_q^{(N)}$ to the thermodynamic limit (assuming that the finite size corrections are polynomial functions of $1/\ln N$ [66]), we extract the fractal dimensions, D_q . The fractal dimensions can at most monotonically decrease with q and are bounded from below by

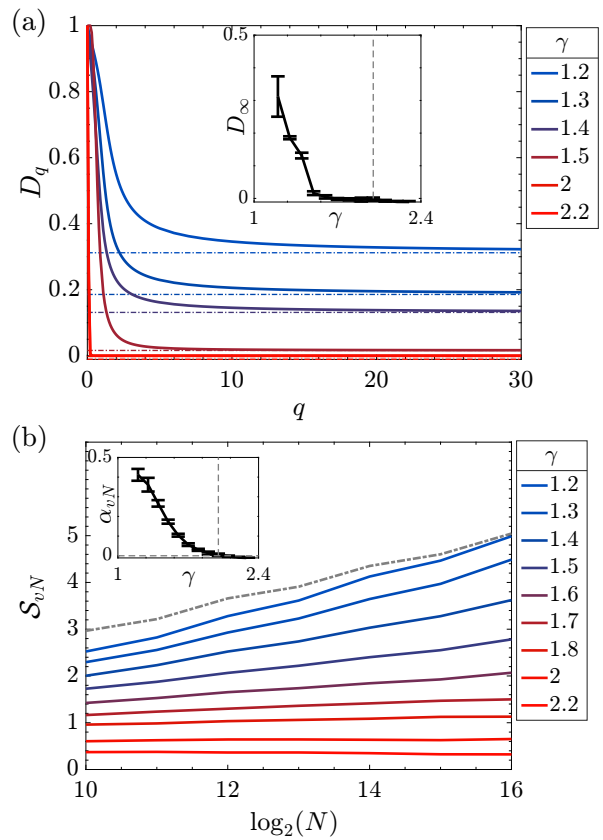


FIG. 3. **Ground state eigenfunctions of sGOE.** (a) Fractal dimensions of the ground state for different values of γ . Horizontal dashed lines denote the smallest fractal dimension, D_∞ . Inset shows D_∞ as a function of γ . (b) Bipartite von Neumann entanglement entropy as a function of system size for various γ . Gray dashed line denotes the Page value [71]. Inset shows the system size scaling $S_{vN} \propto \alpha_{vN} \ln N$. Error bars denote 95% confidence interval.

D_∞ , which determines the scaling of the maximum wavefunction intensity, $\max_n |\Psi(n)|^2 \sim N^{-D_\infty}$ [67, 68]. All the fractal dimensions are unity for an ergodic wavefunction, which is uniformly spread over the Hilbert space irrespective of the choice of basis [69, 70]. On the other hand, $D_q = 0$ for all values of q for a wavefunction localized on the Fock space.

In Fig. 3(a), we show the fractal dimensions for different values of γ . We find that for $\gamma \geq 2$, the fractal dimensions are zero for $q > 0$, indicating that the ground state is localized. Contrarily for $\gamma < 2$, $0 < D_q < 1$ and the fractal dimensions exhibit q -dependence. This implies that different moments of the ground state intensities exhibit distinct scaling exponents, i.e. the ground state is multifractal [65]. Thus, the ground state is non-ergodic but extended for $0 < \gamma < 2$, with an extensively large support set on the Hilbert space but occupies a vanishing fraction of the Hilbert space volume [72–75]. In particular, D_∞ (see the inset of Fig. 3(a)) indicates that a vanishing fraction of the ground state intensities are anomalously large in the delocalized regime. Hence,

localization properties of the ground state indicate that a quantum phase transition occurs at $\gamma = 2$ ($p = N^{-1}$).

To understand the structure of an eigenstate in case of a random matrix, the site basis is the natural choice for computing the IPRs. However, the choice of basis can be ambiguous for a generic nonergodic system. Compared to the localization measures like IPRs, the von Neumann entanglement entropy provides a basis independent analysis of a wavefunction [76–78]. To compute the entanglement measures in case of a random matrix, consider two Hilbert spaces, \mathcal{H}_A and \mathcal{H}_B with dimensions N_A and N_B and spanned by the bases, $\{|a_i\rangle\}$ and $\{|b_j\rangle\}$, respectively. Then, any pure state $|\Psi\rangle$ in the tensor product space $\mathcal{H} \equiv \mathcal{H}_A \otimes \mathcal{H}_B$ can be expressed as [79, 80]

$$|\Psi\rangle = \sum_{i,j} c_{ij} |a_i\rangle \otimes |b_j\rangle \quad (11)$$

where $\{c_{ij}\}$ is a $N_A \times N_B$ matrix. Schmidt decomposition implies that $\{c_{ij}\} = U\Sigma V^*$ ($= U\Sigma V^T$) where U, V are $N_A \times N_A$ and $N_B \times N_B$ unitary (orthogonal) matrices for complex (real) matrix $\{c_{ij}\}$. Σ is a $N_A \times N_B$ diagonal matrix with real non-negative entries, $\{\alpha_k\}_{1 \leq k \leq N'}$, where $N' \leq \min\{N_A, N_B\}$ is the rank of $\{c_{ij}\}$. The Schmidt coefficients, α_k 's are unique up to reordering but U, V are not. Then,

$$|\Psi\rangle = \sum_{k=1}^{N'} \alpha_k |u_k\rangle \otimes |v_k\rangle \quad (12)$$

where $|\Psi\rangle$ is a column vector with elements c_{ij} from Eq. (11) and $|u_k\rangle, |v_k\rangle$ are the column vectors of U, V . $|\Psi\rangle$ is a separable state for $N' = 1$ and entangled state for $N' > 1$. For a pure state $\varrho \equiv |\Psi\rangle\langle\Psi|$, partial trace over \mathcal{H}_A or \mathcal{H}_B gives a matrix with $|\alpha_k|^2 \equiv \lambda_k$ as the diagonal elements. As any N -dimensional Hilbert space \mathcal{H} can be decomposed as a tensor product space $\mathcal{H} \equiv \mathcal{H}_A \otimes \mathcal{H}_B$, where $\mathcal{H}_{A,B}$ corresponds to the subsystems A and B with dimensions N_A and N/N_A , the reduced density matrix of a pure state $|\Psi\rangle$ in \mathcal{H} over subsystem A is $\varrho_A \equiv \text{Tr}_B [|\Psi\rangle\langle\Psi|]$. Then, the von-Neumann entanglement entropy of $|\Psi\rangle$ w.r.t. the subsystem A is [81]

$$\mathcal{S}_{vN} = - \sum_{k=1}^{N'} \lambda_k \ln \lambda_k, \quad N' \leq \min \left\{ N_A, \frac{N}{N_A} \right\} \quad (13)$$

where the diagonal elements of ϱ_A are λ_k . Since $\sum_k \lambda_k = 1$ and $0 < \lambda_k \leq 1$, λ_k 's are distributed over $(N' - 1)$ -dim standard simplex. The eigenvalues of $-\ln \varrho_A$, determines the entanglement spectrum, $\{-\ln \lambda_k\}$.

The entanglement entropy, \mathcal{S}_{vN} quantifies the degree of correlation between the subsystems A and B over a given state. \mathcal{S}_{vN} is 0 for separable states whereas for Haar random vectors, any two subsystems are maximally entangled and the entanglement entropy follows the Page value [71]

$$\mathcal{S}_{vN} \approx \ln N_A - \frac{N_A^2}{2N}, \quad N_A^2 \leq N. \quad (14)$$

The maximal entanglement entropy from Eq. (14) as a function of the subsystem size is known as the Page curve. In Fig. 3(b), we show the bipartite von Neumann entanglement entropy of the ground state of sGOE as a function of system size for different values of γ . We find that the entanglement entropy is independent of system size for $\gamma \geq 2$ while a linear growth $\mathcal{S}_{vN} \sim \alpha_{vN} \log_2 N$ is observed for $\gamma < 2$. The prefactor α_{vN} is shown in the inset of Fig. 3(b) as a function of γ . We find that $0 < \alpha_{vN} < \frac{1}{2}$ for $0 < \gamma < 2$ whereas $\alpha_{vN} \approx \frac{1}{2}$ for an ergodic state. Thus, the entanglement entropy analysis is consistent with our localization measures: the ground state is localized for $\gamma > 2$ and nonergodic extended for $0 < \gamma < 2$, yielding a quantum phase transition at $\gamma = 2$.

IV. DENSITY OF STATES

We begin by calculating the ensemble averaged energy moments whose details are given in Appendix A. Given the density in the matrix space (Eq. (3)) the ensemble average of the second moment of the energy

$$\langle\langle E^2 \rangle\rangle = \frac{1}{N} \left(N + \frac{N(N-1)p}{2} \right) = 1 + \frac{p}{2}(N-1) \quad (15)$$

It is also possible to estimate the ensemble averaged fourth moment of energy for sGOE

$$\langle\langle E^4 \rangle\rangle = \frac{p^2 N^2}{2} + \left(\frac{11}{4}p - \frac{3}{2}p^2 \right) N + \left(p^2 - \frac{11}{4}p + 3 \right) \quad (16)$$

Above equations imply that for $p = N^{-1}$, $\langle\langle E^2 \rangle\rangle \approx \frac{3}{2}$ and $\langle\langle E^4 \rangle\rangle \approx \frac{25}{4}$, provided $N \gg 1$. We numerically obtain the energy moments using the Girard-Hutchinson estimator [82]

$$\text{Tr } H^n \approx \frac{1}{m} \sum_{j=1}^m \langle \Psi_j | H^n | \Psi_j \rangle \quad (17)$$

where $|\Psi_j\rangle$'s are normalized random vectors and $1 \ll m \ll N$. The above stochastic sampling allows us to obtain the energy moments without doing exact diagonalization of H . We checked that the numerically obtained energy moments have a nice agreement with our analytical expressions.

Based on the 2nd and 4th moments of energy, we define the *shifted kurtosis*

$$K = \frac{\langle E^4 \rangle}{\langle E^2 \rangle^2} - 2. \quad (18)$$

The kurtosis allows us to quantify the change in the shape of the density of states (DOS)

$$\rho(E) = \frac{1}{N} \sum_{i=1}^N \delta(E - E_i) \quad (19)$$

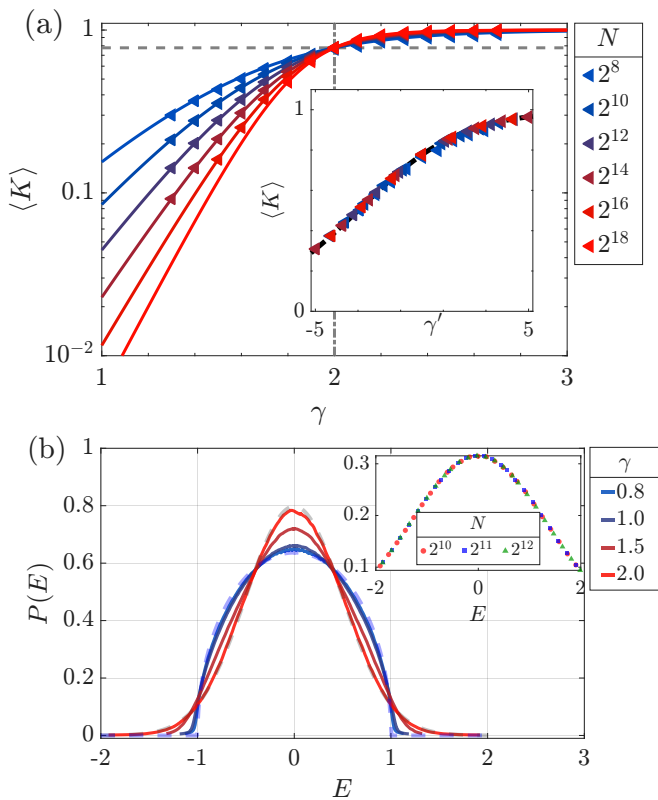


FIG. 4. **Energy moments and DOS of sGOE.** (a) shifted kurtosis (Eq. (18)) as a function of γ for different system sizes (values given in the legend) where sparsity $p \equiv N^{-\frac{1}{2}}$. Markers denote numerical data obtained using Girard-Hutchinson estimator (Eq. (17)) and the solid lines denote the analytical expressions from Eq. (20). Horizontal dashed line correspond to $\langle K \rangle = \frac{25}{4}$. The inset shows the collapsed data assuming 2nd order transition ansatz (Eq. (21)) where $\gamma' \equiv (\gamma - 2) \ln N^{\frac{1}{\nu}}$, $\nu \approx 1.0464$. (b) ensemble averaged DOS obtained using the Lanczos method [83] for $N = 1024$ and different values of γ . We fix the energy variance $\sigma_E^2 = \frac{1}{4}$ for all values of γ . Dashed red (blue) curve denotes the Gaussian (semicircle) distribution. Inset shows the average DOS at $\gamma = 2$ for different system sizes.

where $\{E_j\}$ are the N number of energy levels of a system. The DOS measures the number of available energy eigenstates in a given energy window. In case of a Gaussian (semicircle) DOS, the kurtosis has a value $K = 1$ ($K = 0$). Thus, we expect the kurtosis to interpolate between 0 and 1 as we increase the sparsity of a random matrix from sGOE. The analytical expressions of the energy moments give us

$$K = \frac{4 - p(N-1)(2p-3)}{(2 + (N-1)p)^2} \quad (20)$$

For $p = N^{-1}$, $K = \frac{7}{9}$ is independent of the system size in the limit $N \rightarrow \infty$. In Fig. 4(a), we show the numerically obtained kurtosis along with the analytical expression in Eq. (20) as a function of γ and find a good agreement.

In the inset of Fig. 4(a), we show that the kurtosis data from different system sizes can be collapsed assuming the 2nd order transition ansatz [74, 84–86]

$$\mathbb{O}(\gamma, N) = f((\gamma - \gamma_c) [\ln N]^{\frac{1}{\nu}}) \quad (21)$$

where \mathbb{O} is the observable of our interest, f is an universal function, γ_c and ν are the critical parameter and exponents, respectively. Thus, the DOS of sGOE should be independent of the system size at $\gamma = 2$ (i.e. $p = N^{-1}$), which we verify next.

In the limit $p = 0$, a matrix from sGOE belongs to the Poisson ensemble and the corresponding average DOS follows a Gaussian distribution

$$\langle \rho^P(E) \rangle = \frac{1}{\sqrt{2\pi}\sigma_E} \exp\left(-\frac{E^2}{2\sigma_E^2}\right) \quad (22)$$

where

$$\sigma_E^2 \equiv \langle E^2 \rangle - \langle E \rangle^2 \quad (23)$$

is the energy variance. On the other hand, for $p = 1$, we obtain a matrix from the GOE, where the average DOS follows the Wigner's semicircle law for $N \rightarrow \infty$

$$\rho^{\text{SC}}(E) = \frac{\sqrt{4\sigma_E^2 - E^2}}{2\pi\sigma_E^2}. \quad (24)$$

For finite N , the DOS of GOE can be expressed in terms of the Hermite polynomials [87], with a deviation at the edge of the spectrum from the above semicircle law. Nevertheless, $\rho^{\text{SC}}(E)$ well approximates the average DOS in the bulk energy spectrum of the GOE for $N \gg 1$. In case of sGOE, we expect the average DOS to interpolate between the semicircle law (Eq. (24)) and the Gaussian distribution (Eq. (22)) as we increase the sparsity parameter.

We numerically estimate the ensemble averaged DOS using the kernel polynomial method (KPM) [88–90]. First, we estimate the lower and upper energy bounds using a partial Lanczos reduction of the input matrix H [83]. Then, we scale and shift H to ensure the energy levels are within $[-1, 1]$. Next, we expand the DOS w.r.t. the Chebyshev polynomials of 1st kind, $T_j(x)$

$$\rho(\tilde{E}) = \frac{1}{\sqrt{1 - \tilde{E}^2}} \sum_{j=0}^{\infty} \mu_j T_j(\tilde{E}) \quad (25)$$

where $-1 \leq \tilde{E} \leq 1$ is the shifted and scaled energy. The Chebyshev moments, μ_j 's are uniquely related to the energy moments due to the orthogonality of the Chebyshev polynomials. For example,

$$\langle \tilde{E}^2 \rangle = \frac{1}{2} + \frac{\pi\mu_2}{4}, \quad \langle \tilde{E}^4 \rangle = \frac{3}{8} + \frac{\pi\mu_2}{4} + \frac{\pi\mu_4}{16} \quad (26)$$

To numerically estimate the DOS, we truncate the series in Eq. (25) to a finite order and estimate the μ_j 's using

a stochastic sampling as in Eq. (17). Such a truncation leads to a Gibbs oscillation in the estimated DOS which is a sum of delta functions. We convolve the DOS with the Jackson kernel to get rid of the Gibbs oscillation [88]. We find that despite Jackson damping, the estimated DOS tends to have negative values close to the edges of the spectrum.

To avoid the unphysical situation where the DOS becomes negative, we use the Lanczos method [83, 91] to estimate the DOS. We perform a partial Lanczos reduction of H w.r.t. a random vector to obtain the Ritz values and vectors. A weighted histogram of the Ritz values w.r.t. the 1st squared components of the Ritz vectors gives an estimate of the DOS.

In Fig. 4(b), we show the ensemble averaged DOS for different values of γ obtained using the Lanczos method. The obtained DOS is always positive in contrast to the KPM. Note that, the DOS can also be obtained by numerically solving the Hammerstein equations, as shown for the adjacency and Laplacian matrices of the Erdős-Rényi-Gilbert graph in Ref. [92].

In the inset of Fig. 4(b), we show the average DOS for $\gamma = 2$ and different system sizes. We find that the DOS is independent of N , as predicted by the shifted kurtosis in Eq. (20). We compared the numerically obtained DOS of sGOE with the analytical DOS of other notable random matrix models, e.g. Rosenzweig-Porter ensemble [93], banded random matrices [94], β -ensemble [95]. We do not find an one-to-one correspondence of the sGOE with any of the above random matrix models in terms of the average DOS, as the crossover from the semi-circle to the Gaussian DOS is not universal.

V. ENERGY CORRELATIONS

The energy levels of a matrix from GOE are correlated at all possible length scales, which is a characteristic signature of quantum chaos [96]. Contrarily, the energy levels of the Poisson ensemble remain uncorrelated as conjectured for an integrable quantum system [97]. In case of sGOE, we intuitively expect that the energy correlations get suppressed as we increase the sparsity of the random matrix. To quantify the nature of short-range energy correlation (i.e. on the scale of mean level spacing), we look at the distribution of level spacings, $s_j \equiv \mathcal{E}_{j+1} - \mathcal{E}_j$, where $\{\mathcal{E}_j\}$ is the unfolded spectrum [98, 99]. For unfolded spectrum, the DOS becomes uniform such that the mean position of the j th unfolded energy level $\langle \mathcal{E}_j \rangle = j$. In case of the Poisson ensemble, the density of level spacings follows an exponential distribution, $P_{\text{Poisson}}(s) = e^{-s}$ while for GOE, the density of level spacing is well approximated by the Wigner's surmise [100]. The Wigner's surmise implies that $P_{\text{GOE}}(s \rightarrow 0) \rightarrow 0$, i.e. the energy levels cannot come arbitrarily close to each other, a property known as the *level repulsion*, which is typically observed in chaotic quantum systems [96, 101, 102].

We find that for small values of sparsity γ , the density

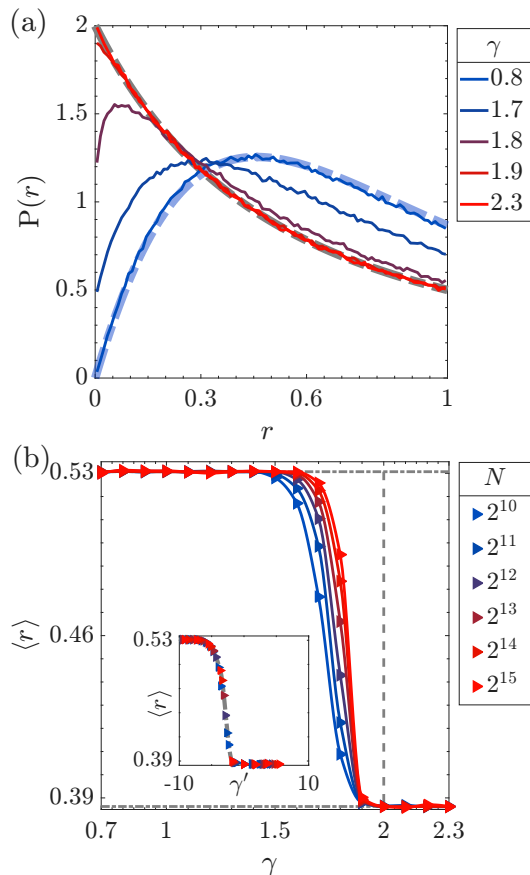


FIG. 5. **Short-range energy correlation of sGOE.** (a) density of the ratio of level spacings for middle 40% spectrum, $N = 1024$ and different values of γ . Dashed blue (red) curve denotes the analytical expressions of GOE (Poisson ensemble). (b) average ratio of level spacings as a function of γ for different system sizes. Inset shows the collapsed data following Eq. (21) for a critical parameter $\gamma_c = 2$ and exponent $\nu \approx 0.9316$.

of level spacings $P(s)$ follows that of the GOE, while upon increasing γ the density converges to that of the Poisson ensemble [103].

To quantify such a crossover and ensuring that our analysis of the short-range correlation is not affected by the unfolding process [104], we look at the ratio of level spacings [105, 106]

$$r_j = \min\left(\tilde{r}_j, \frac{1}{\tilde{r}_j}\right), \quad \tilde{r}_j \equiv \frac{E_{j+1} - E_j}{E_j - E_{j-1}}. \quad (27)$$

In case of the GOE and the Poisson ensemble, the density of the ratio of level spacings follows [106]

$$P_{\text{GOE}}(r) = \frac{27}{4} \frac{r + r^2}{(1 + r + r^2)^{\frac{5}{2}}} \quad (28)$$

$$P_{\text{Poisson}}(r) = \frac{2}{(1+r)^2}, \quad 0 \leq r \leq 1.$$

In Fig. 5(a), we show the density of the ratio of level spacings for the middle 40% energy spectrum for $N = 1024$

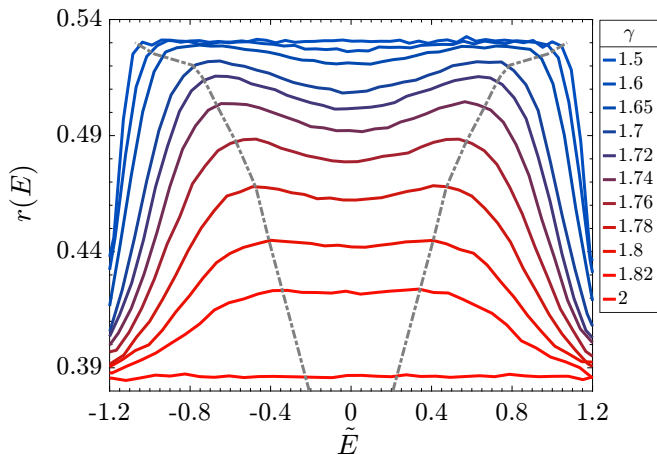


FIG. 6. **Mobility edge.** Ratio of level spacing as a function of energy for $N = 4096$ and different values of γ . $\tilde{E} = E/2\sigma_E$ denotes the scaled energy. Gray dashed lines denote the mobility edges.

and different values of γ along with the above analytical expressions. We find that $P(r)$ interpolates between the GOE and Poisson limit as we increase γ and to quantify such interpolation, we look at the average ratio of level spacing, $\langle r \rangle$. From the analytical expressions in Eq. (28), we can calculate the average ratio of level spacing to be $\langle r \rangle^{\text{GOE}} \approx 0.53$ and $\langle r \rangle^{\text{Poisson}} \approx 0.39$ for the GOE and Poisson ensemble, respectively [106].

In Fig. 5(b), we show the average ratio of level spacing as a function of γ for different system sizes. Corresponding inset shows the collapsed data following Eq. (21). Thus, both the level spacing and its ratio indicate that the short-range energy correlation in the bulk spectrum of sGOE undergoes a 2nd order phase transition at $\gamma = 2$ (i.e. sparsity, $p = N^{-1}$) such that there is no correlation among the neighboring bulk energy levels for $\gamma > 2$.

A. Mobility edge

The adjacency matrix of the Erdős-Rényi-Gilbert graph [26] as well as its weighted version [27] exhibits mobility edge, i.e. a critical energy separating the localized low-energy eigenstates from the extended excited states. We are interested to know if the addition of on-site disorder affects the presence of the mobility edge in the delocalized phase of sparse random matrices. For localized eigenstates, the energy levels are uncorrelated whereas the extended states hybridize among themselves, producing correlated spectrum. Thus, by looking at the short-range correlation measures as a function of energy, we can identify the mobility edge.

In particular, we look at the ratio of level spacing as a

function of energy [107]

$$r(E) = \frac{1}{N\rho(E)} \sum_{n=1}^N r_n \delta(E - E_n) \quad (29)$$

$$r_n = \min\left(\tilde{r}_n, \frac{1}{\tilde{r}_n}\right), \quad \tilde{r}_n = \frac{E_{n+1} - E_n}{E_n - E_{n-1}}$$

In Fig. 6, we show the energy dependence of the ratio of level spacing for $N = 4096$ and various values of γ . The energy axis is scaled as $\tilde{E} = E/2\sigma_E$ to ensure that the spectral width is independent of γ . We identify the mobility edge as the energy where $r(E)$ deviates from its bulk behavior. As shown in Fig. 6, the mobility edges (gray dashed curves) shrink towards zero energy as we increase γ . For $\gamma > 2$, the ratio of level spacing is homogeneous over the spectrum and reaches the Poisson limit. Thus, we find that despite the addition of the on-site disorder, the mobility edge survives in the delocalized phase of the sparse random matrices.

B. Long-range energy correlations

Now, we look at the correlation between two energy levels which are far apart from each other. In a series of seminal works, Dyson showed that the energy levels of the Wigner-Dyson ensembles can be interpreted as the equilibrium configuration of Coulomb gas particles confined on a line at a temperature inversely proportional to the degree of level repulsion [108, 109]. Thus, for a fixed N , upon decreasing the temperature (i.e. increasing the degree of level repulsion), the Coulomb gas particles freeze to their respective mean positions and produce a picket-fence spectrum [110–112]. As we increase the temperature of the Coulomb gas, in the analogous energy spectrum, the energy levels can fluctuate more around their mean positions and eventually describe a Poisson process where all the energy correlations are lost [74, 95, 107].

The fluctuation of the n th unfolded energy level, \mathcal{E}_n around its mean position, $\langle \mathcal{E}_n \rangle = n$ can be expressed as

$$\delta_n \equiv \mathcal{E}_n - n = \sum_{k=1}^N c_k \Psi_k(n) \quad (30)$$

where $\{\omega_k, |\Psi_k\rangle\}$ is an eigenpair of the correlation matrix

$$C_{mn} = \langle \mathcal{E}_m \mathcal{E}_n \rangle - \langle \mathcal{E}_m \rangle \langle \mathcal{E}_n \rangle. \quad (31)$$

$|\Psi_k\rangle$ is the k th normal mode of the energy level fluctuations with a wavelength $\sim \mathcal{O}(k^{-1})$ and mean square amplitude ω_k [103, 113]. Then, ω_k as a function of the wavenumber k gives the dispersion relation of the normal modes. In particular, the normal mode $|\Psi_1\rangle$ with the longest wavelength describes the collective motion where all the energy levels have a common shift without any change in the relative distances. For GOE, $\omega_k \propto k^{-1}$ and for Poisson ensemble, $\omega_k \propto k^{-2}$ and corresponding normal modes are called rigid and soft respectively. Rigid

short (long)-wavelength modes indicate the presence of short (long)-range energy correlations. Thus, the dispersion relation of the energy level fluctuations reflects the nature of energy correlations across all possible length scales.

1. Level Number Variance

To understand the long-range energy correlations in case of the sGOE, we compute the number variance [114]

$$\Sigma^2(\Delta\mathcal{E}) = \left\langle [\mathcal{N}(\mathcal{E}_0, \Delta\mathcal{E}) - \Delta\mathcal{E}]^2 \right\rangle_{\mathcal{E}_0} \quad (32)$$

$$\mathcal{N}(\mathcal{E}_0, \Delta\mathcal{E}) = I\left(\mathcal{E}_0 + \frac{\Delta\mathcal{E}}{2}\right) - I\left(\mathcal{E}_0 - \frac{\Delta\mathcal{E}}{2}\right)$$

where $I(\mathcal{E})$ is the cumulative distribution of the unfolded energy levels, $\mathcal{N}(\mathcal{E}_0, \Delta\mathcal{E})$ is the number of energy levels in the window of span $\Delta\mathcal{E}$ and centered at \mathcal{E}_0 . In case of GOE, the number variance behaves as [98]

$$\Sigma_{\text{GOE}}^2(\Delta\mathcal{E}) \approx \frac{2}{\pi^2} \left(\ln(2\pi\Delta\mathcal{E}) + \gamma_E + 1 - \frac{\pi^2}{8} \right) \quad (33)$$

where $\gamma_E = 0.577216\dots$ is the Euler-Mascheroni constant. The logarithmic behavior of the number variance (Eq. (33)) is a consequence of the *rigidity* of the energy spectrum where the fluctuations of an energy level from its average position over different disorder realizations are restricted due to the correlations with the rest of the spectrum.

In contrast, the number variance of the Poisson ensemble has a linear behavior, $\Sigma^2(\Delta\mathcal{E}) = \Delta\mathcal{E}$, indicating the absence of correlation at any length scale.

In various disordered single-particle [115–117], many-body [118–122], random matrix models [72, 94, 123, 124], there exists a mesoscopic energy scale called the *Thouless energy*, E_{Th} [125–127], below which the energy levels are correlated similar to the GOE and exhibit universal statistical properties. On the other hand, two energy levels with gap larger than E_{Th} can be either weakly correlated [128–130] or completely uncorrelated such that

$$\Sigma^2(\Delta\mathcal{E}) \propto \begin{cases} \frac{2}{\pi^2} \log \Delta\mathcal{E}, & \Delta\mathcal{E} < E_{\text{Th}} \\ \Delta\mathcal{E}, & \Delta\mathcal{E} > E_{\text{Th}} \end{cases}. \quad (34)$$

Thus, comparing the number variance of an energy spectrum with that of the GOE (Eq. (33)), one can estimate the Thouless energy scale. Ref. [103] showed that for $pN \sim \mathcal{O}(1)$, the long-range correlation is homogeneous in the bulk spectrum of sGOE. In Fig. 7(a), we show the ensemble averaged number variance as a function of the energy gap for different values of γ and observe a crossover from a logarithmic to a linear behavior as we increase γ .

We identify the unfolded Thouless energy scale via markers beyond which the number variance deviates from

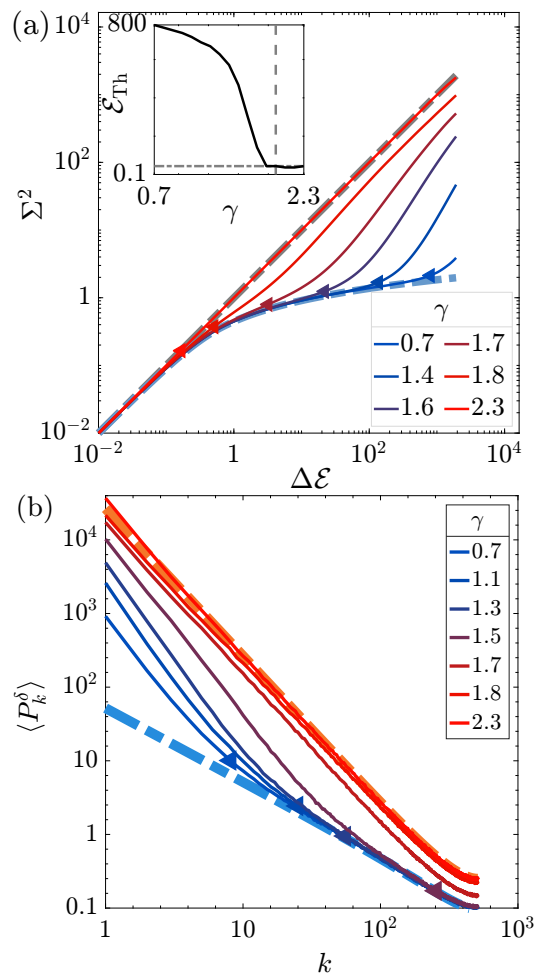


FIG. 7. **Long-range energy correlation of sGOE.** (a) Number variance as a function of energy gap for $N = 16384$ and different values of γ . Markers denote the unfolded Thouless energy, \mathcal{E}_{Th} . Dashed blue (gray) curve denotes the analytical expression of GOE (Poisson ensemble) given in Eq. (33). Inset shows the unfolded Thouless energy as a function of γ . (b) Ensemble averaged power-spectrum of noise for $N = 1024$ and different values of γ . Dashed blue (red) curve denotes the analytical expression of GOE (Poisson ensemble). Markers denote the Thouless frequency $k_{\text{Th}} = N/\mathcal{E}_{\text{Th}}$.

$\Sigma_{\text{GOE}}^2(\Delta\mathcal{E})$ (Eq. (33)) by a threshold value. In the inset of Fig. 7(a), we show that the Thouless energy is constant for $\gamma > 2$ and increases monotonically for $\gamma < 2$ as we decrease γ . We observe that for $\gamma \geq 2$ the Thouless energy $\mathcal{E}_{\text{Th}} \sim \mathcal{O}(1)$ is independent of the system size, implying uncorrelated spectrum across all possible length scales. In contrast, the Thouless energy is an extensive quantity for $\gamma < 2$, below which the energy correlations follow the universal features predicted by the random matrix theory.

2. Power Spectrum

We can probe the nature of long-range energy correlation in the frequency space by computing the power-spectrum of the δ_n statistics [131, 132]

$$P_k^\delta = |\hat{\delta}_k|^2, \quad \hat{\delta}_k = \frac{1}{\sqrt{N}} \sum_n \delta_n \exp\left(-\frac{i2\pi kn}{N}\right) \quad (35)$$

The ensemble averaged power-spectrum exhibits a homogeneous linear decay w.r.t. the positive frequencies in case of the GOE whereas the decay is quadratic in Poisson ensembles. However, the power-spectrum exhibits a heterogeneous behavior separated by a critical frequency, k_{Th} , in systems with a well-defined Thouless energy E_{Th} , for e.g. disordered Heisenberg spin-chain [122, 133], Rosenzweig-Porter ensemble [74, 134]. As the frequency is Fourier dual to the energy, the presence of GOE like energy correlation below E_{Th} should be reflected in the linear dependence of the high-frequency $\langle P_k^\delta \rangle$ for $k > k_{\text{Th}}$. On the other hand, the absence of energy correlation above E_{Th} should lead to a quadratic behavior of the low-frequency power-spectrum for $k < k_{\text{Th}}$. Thus, we expect the following heterogeneous behavior for sGOE

$$\langle P_k^\delta \rangle \propto \begin{cases} k^{-2}, & k < k_{\text{Th}} \\ k^{-1}, & k > k_{\text{Th}} \end{cases}, \quad k_{\text{Th}} \sim \frac{N}{\mathcal{E}_{\text{Th}}}. \quad (36)$$

Note that, a complimentary heterogeneous behavior is found in the nonergodic phase of the β -ensemble [74, 95, 107], banded random matrix [94], where anomalous long-range energy correlations exist despite the absence of any short-range correlation.

In Fig. 7(b), we show the ensemble averaged power-spectrum of noise for $N = 1024$ and different values of γ along with the analytical expressions of the GOE and Poisson ensemble [131]. We find that for $\gamma > 2$, the power-spectrum exhibits a quadratic decay for all frequencies and is well described by the Poisson expression, indicating the absence of energy correlations at all length scales.

On the other hand, for small values of γ , the power-spectrum follows the GOE expression at high frequencies but deviates from the linear decay below the Thouless frequency (shown by markers in Fig. 7(c)). This confirms our conclusions from the number variance, i.e. for $0 < \gamma < 2$, there is energy correlation below the Thouless energy scale while the long-range correlations are absent.

VI. DISCUSSIONS

In this work, we investigated the effects of diagonal disorder in a sparse random matrix ensemble analogous to the adjacency matrix of a weighted Erdős-Rényi graph. Consistent with earlier studies [27], we obtained the localization-transition at the critical percolation limit $\gamma = 2$ (where the sparsity is parameterized

as $p = N^{-\gamma/2}$), even in the presence of diagonal disorder. By analyzing the structure of the ground state through generalized IPR and bipartite entanglement entropy, we observed a multifractal NEE ground state for $0 < \gamma < 2$ while the ground state was found to be localized for $\gamma > 2$, implying quantum phase transition at $\gamma = 2$. The density of states exhibits a transition from the Wigner semicircle to a Gaussian (Poisson-like) form with increasing γ .

We analytically calculated the second and fourth energy moments of the ensemble and using this, we showed that the shifted kurtosis exhibits a typical second order transition at $\gamma = 2$. Furthermore, we numerically showed a mobility edge separating extended and localized eigenstates persists even in the presence of diagonal disorder.

An analysis of long-range spectral correlations showed characteristics of typical interacting many-body systems, indicating the presence of a Thouless energy scale E_{Th} . This behaviour is also reflected in the power spectrum, which shows distinct scaling regimes above and below a characteristic frequency k_{Th} . Our results are particularly important as recently, for a sparse Sachdev-Ye-Kitaev model, the dynamics of the real part of the survival amplitude of an initial state has been experimentally simulated on an ion trap quantum computer [135]. For future work, we can probe the dynamical behavior through the spectral form factor and survival probability in order to identify the relevant timescales in sparse random matrix ensembles.

ACKNOWLEDGMENTS

We acknowledge the support from the Kepler Computing facility, maintained by the Department of Physical Sciences, IISER Kolkata, for various computational needs. A. K. D. acknowledges support from the Leverhulme Trust Research Project Grant RPG-2025-063.

Appendix A: Energy moments

The density in the matrix space (Eq. (3)) allows us to obtain the ensemble averaged energy moments. Specifically, $\langle E^n \rangle = \frac{1}{N} \text{Tr} H^n$ due to cyclic property of the trace [136]. Then,

$$\langle \langle E^n \rangle \rangle = \frac{1}{N} \int dH \mathcal{P}(H) \text{Tr} H^n \quad (A1)$$

where $\langle \langle \dots \rangle \rangle$ implies an average over the energy spectrum as well as the ensemble of H . From the symmetry of H we obtain,

$$\text{Tr} H^2 = \sum_i H_{ii}^2 + 2 \sum_{i < j} H_{ij}^2 \quad (A2)$$

Equation (2) implies that the diagonal elements are random variables with unit variance and the non-zero off-diagonal elements are random variables with variance $\frac{1}{2}$.

Thus, ensemble average of the above trace is

$$\begin{aligned} \langle \text{Tr } H^2 \rangle &= \sum_i 1 + 2 \sum_{i < j} \left((1-p) \times 0 + p \times \frac{1}{2} \right) \\ &= N + 2 \times \frac{N(N-1)}{2} \times \frac{p}{2} \\ &= N + \frac{N(N-1)p}{2} \end{aligned} \quad (\text{A3})$$

Hence, the ensemble averaged 2nd moment of the energy is

$$\langle E^2 \rangle = \frac{1}{N} \left(N + \frac{N(N-1)p}{2} \right) = 1 + \frac{p}{2}(N-1) \quad (\text{A4})$$

The 4th moment of the energy is $\langle E^4 \rangle = \frac{1}{N} \text{Tr } H^4$. Note that,

$$\begin{aligned} \text{Tr } H^4 &= \text{Tr} \left(H^2 \cdot H^2 \right) = \sum_a (H^2 \cdot H^2)_{aa} \\ &= \sum_{a,b} (H^2)_{ab} (H^2)_{ba} = \sum_{a,b} [(H^2)_{ab}]^2 \end{aligned} \quad (\text{A5})$$

For the diagonal elements ($a = b = i$), we get

$$\begin{aligned} \langle [(H^2)_{ii}]^2 \rangle &= \left\langle \left[\sum_k H_{ik}^2 \right]^2 \right\rangle = \sum_k \langle H_{ik}^4 \rangle + \sum_{k \neq l} \langle H_{ik}^2 H_{il}^2 \rangle \\ &= \sum_k \langle H_{ik}^4 \rangle + \sum_{k \neq l} \langle H_{ik}^2 \rangle \langle H_{il}^2 \rangle \end{aligned} \quad (\text{A6})$$

For the first term, if $k = i$ we have $\langle H_{ii}^4 \rangle = 3$ from the 4th moment of the Gaussian distribution. Contrarily, if $k \neq i$, we have $N-1$ terms, each having a value $(1-p) \times 0 + p \times (3 \cdot \frac{1}{4}) = \frac{3}{4}p$. Note that, the second term can be

written as

$$\begin{aligned} \sum_{k \neq l} \langle H_{ik}^2 \rangle \langle H_{il}^2 \rangle &= \left[\sum_k \langle H_{ik}^2 \rangle \right]^2 - \sum_k \langle H_{ik}^2 \rangle^2 \\ &= \left[1 + \frac{p}{2}(N-1) \right]^2 - \left[1 + (N-1) \frac{p^2}{4} \right] \end{aligned}$$

Thus, for the diagonal terms, we get a total contribution of

$$N \left[3 + (N-1) \frac{3p}{4} + \left(1 + \frac{p}{2}(N-1) \right)^2 - \left(1 + (N-1) \frac{p^2}{4} \right) \right] \quad (\text{A7})$$

For the off-diagonal terms, $a = i \neq b = l$ we have:

$$\begin{aligned} \langle [(H^2)_{il}]^2 \rangle &= \langle H_{il}^2 H_{il}^2 \rangle = \left\langle \left(\sum_k H_{ik} H_{kl} \right) \left(\sum_r H_{ir} H_{rl} \right) \right\rangle \\ &= \sum_{k,r} \langle H_{ik} H_{kl} H_{ir} H_{rl} \rangle \end{aligned} \quad (\text{A8})$$

If $k \neq r$, as $i \neq l$ all terms become independent and vanish, since mean of the entries is zero. So, we consider only $k = r$ case:

- $k = r = i$ or $k = r = l$

$$\langle H_{ii}^2 H_{il}^2 \rangle = 1 \times \frac{p}{2} \quad \langle H_{il}^2 H_{ll}^2 \rangle = 1 \times \frac{p}{2}$$

- $k = r \neq i, l$

$$\sum_{k \neq i, l} \langle H_{ik}^2 H_{kl}^2 \rangle = (N-2) \times \frac{p}{2} \times \frac{p}{2} = (N-2) \frac{p^2}{4}$$

Thus, for the off-diagonal terms, we obtain a total contribution of,

$$\left[p + (N-2) \frac{p^2}{4} \right] \times N(N-1) \quad (\text{A9})$$

Adding both the contributions from Eqs. (A7) and (A9), we obtain the ensemble averaged fourth moment of energy for sGOE

$$\langle \langle E^4 \rangle \rangle = \frac{p^2 N^2}{2} + \left(\frac{11}{4}p - \frac{3}{2}p^2 \right) N + \left(p^2 - \frac{11}{4}p + 3 \right) \quad (\text{A10})$$

[1] A. M. Kaufman, M. E. Tai, A. Lukin, M. Rispoli, R. Schittko, P. M. Preiss, and M. Greiner, Quantum thermalization through entanglement in an isolated

many-body system, *Science* **353**, 794 (2016).

[2] P. Richerme, Z.-X. Gong, A. Lee, C. Senko, J. Smith, M. Foss-Feig, S. Michalakis, A. V. Gorshkov, and

- C. Monroe, Non-local propagation of correlations in quantum systems with long-range interactions, *Nature* **511**, 198 (2014).
- [3] H. Dong, P. Zhang, C. B. Dağ, Y. Gao, N. Wang, J. Deng, X. Zhang, J. Chen, S. Xu, K. Wang, Y. Wu, C. Zhang, F. Jin, X. Zhu, A. Zhang, Y. Zou, Z. Tan, Z. Cui, Z. Zhu, F. Shen, T. Li, J. Zhong, Z. Bao, H. Li, Z. Wang, Q. Guo, C. Song, F. Liu, A. Chan, L. Ying, and H. Wang, Measuring the spectral form factor in many-body chaotic and localized phases of quantum processors, *Phys. Rev. Lett.* **134**, 010402 (2025).
- [4] K. X. Wei, C. Ramanathan, and P. Cappellaro, Exploring localization in nuclear spin chains, *Phys. Rev. Lett.* **120**, 070501 (2018).
- [5] D. M. Basko, I. L. Aleiner, and B. L. Altshuler, Metal-insulator transition in a weakly interacting many-electron system with localized single-particle states, *Annals of physics* **321**, 1126 (2006).
- [6] A. Pal and D. A. Huse, Many-body localization phase transition, *Phys. Rev. B* **82**, 174411 (2010).
- [7] R. Nandkishore and D. A. Huse, Many-body localization and thermalization in quantum statistical mechanics, *Annu. Rev. Condens. Matter Phys.* **6**, 15 (2015).
- [8] M. Serbyn and J. E. Moore, Spectral statistics across the many-body localization transition, *Phys. Rev. B* **93**, 041424 (2016).
- [9] E. Chertkov, B. Villalonga, and B. K. Clark, Numerical evidence for many-body localization in two and three dimensions, *Phys. Rev. Lett.* **126**, 180602 (2021).
- [10] I. Vallejo-Fabila, A. K. Das, D. A. Zarate-Herrada, A. S. Matsoukas-Roubeas, E. J. Torres-Herrera, and L. F. Santos, Reducing dynamical fluctuations and enforcing self-averaging by opening many-body quantum systems, *Phys. Rev. B* **110**, 075138 (2024).
- [11] I. Vallejo-Fabila, A. K. Das, S. Choudhury, and L. F. Santos, Single-site measurements as probes of many-body quantum chaos, *Phys. Rev. E* **112**, 044208 (2025).
- [12] A. K. Das and A. Lazarides, Ground state and persistent oscillations in the quantum east model (2026), arXiv:2602.23422 [quant-ph].
- [13] B. L. Altshuler, Y. Gefen, A. Kamenev, and L. S. Levitov, Quasiparticle lifetime in a finite system: A nonperturbative approach, *Phys. Rev. Lett.* **78**, 2803 (1997).
- [14] M. Tarzia, Many-body localization transition in hilbert space, *Phys. Rev. B* **102**, 014208 (2020).
- [15] S. Roy and D. E. Logan, Fock-space correlations and the origins of many-body localization, *Phys. Rev. B* **101**, 134202 (2020).
- [16] V. Kravtsov, B. Altshuler, and L. Ioffe, Non-ergodic delocalized phase in anderson model on bethe lattice and regular graph, *Annals of Physics* **389**, 148 (2018).
- [17] G. De Tomasi, S. Bera, A. Scardicchio, and I. M. Khaymovich, Subdiffusion in the anderson model on the random regular graph, *Phys. Rev. B* **101**, 100201 (2020).
- [18] B. Saha and S. Roy, Anderson localisation in spatially structured random graphs (2026), arXiv:2601.00220 [cond-mat.dis-nn].
- [19] N. Macé, F. Alet, and N. Laflorencie, Multifractal scalings across the many-body localization transition, *Phys. Rev. Lett.* **123**, 180601 (2019).
- [20] G. De Tomasi, I. M. Khaymovich, F. Pollmann, and S. Warzel, Rare thermal bubbles at the many-body localization transition from the fock space point of view, *Phys. Rev. B* **104**, 024202 (2021).
- [21] C. Monthus and T. Garel, Anderson localization on the cayley tree: multifractal statistics of the transmission at criticality and off criticality, *Journal of Physics A: Mathematical and Theoretical* **44**, 145001 (2011).
- [22] M. Sonner, K. S. Tikhonov, and A. D. Mirlin, Multifractality of wave functions on a cayley tree: From root to leaves, *Phys. Rev. B* **96**, 214204 (2017).
- [23] P. A. Nosov, I. M. Khaymovich, A. Kudlis, and V. E. Kravtsov, Statistics of Green's functions on a disordered Cayley tree and the validity of forward scattering approximation, *SciPost Phys.* **12**, 048 (2022).
- [24] P. Erdős and A. Rényi, On random graphs i., *Publ. math. debrecen* **6**, 18 (1959).
- [25] E. N. Gilbert, Random graphs, *The Annals of Mathematical Statistics* **30**, 1141 (1959).
- [26] J. Alt, R. Ducatez, and A. Knowles, Delocalization transition for critical Erdős-Rényi graphs, *Communications in Mathematical Physics* **388**, 507 (2021).
- [27] L. F. Cugliandolo, G. Schehr, M. Tarzia, and D. Venturelli, Multifractal phase in the weighted adjacency matrices of random Erdős-Rényi graphs, *Phys. Rev. B* **110**, 174202 (2024).
- [28] A. Khorunzhy and G. Rodgers, On the wigner law in dilute random matrices, *Reports on Mathematical Physics* **42**, 297 (1998).
- [29] G. J. Rodgers and A. J. Bray, Density of states of a sparse random matrix, *Phys. Rev. B* **37**, 3557 (1988).
- [30] Y. V. Fyodorov and A. D. Mirlin, Localization in ensemble of sparse random matrices, *Phys. Rev. Lett.* **67**, 2049 (1991).
- [31] S. Roy and A. Lazarides, Strong ergodicity breaking due to local constraints in a quantum system, *Phys. Rev. Res.* **2**, 023159 (2020).
- [32] A. K. Das, C. Cianci, D. G. A. Cabral, D. A. Zarate-Herrada, P. Pinney, S. Pilatowsky-Cameo, A. S. Matsoukas-Roubeas, V. S. Batista, A. del Campo, E. J. Torres-Herrera, and L. F. Santos, Proposal for many-body quantum chaos detection, *Phys. Rev. Res.* **7**, 013181 (2025).
- [33] P. Lydzba, Y. Zhang, M. Rigol, and L. Vidmar, Single-particle eigenstate thermalization in quantum-chaotic quadratic hamiltonians, *Phys. Rev. B* **104**, 214203 (2021).
- [34] D. S. Dean, An approximation scheme for the density of states of the laplacian on random graphs, *Journal of Physics A: Mathematical and General* **35**, L153 (2002).
- [35] J.-Y. Fortin, Asymptotic behaviour of the density of states on a random lattice, *Journal of Physics A: Mathematical and General* **38**, L57 (2005).
- [36] R. Kühn, Spectra of sparse random matrices, *Journal of Physics A: Mathematical and Theoretical* **41**, 295002 (2008).
- [37] T. Rogers, I. P. Castillo, R. Kühn, and K. Takeda, Cavity approach to the spectral density of sparse symmetric random matrices, *Phys. Rev. E* **78**, 031116 (2008).
- [38] V. A. R. Susca, P. Vivo, and R. Kühn, Cavity and replica methods for the spectral density of sparse symmetric random matrices, *SciPost Phys. Lect. Notes* , 33 (2021).
- [39] A. Khorunzhy and G. Rodgers, Eigenvalue distribution of large dilute random matrices, *Journal of Mathematical Physics* **38**, 3300 (1997).
- [40] A. Khorunzhy, On dilute unitary random matrices, *Journal of Physics A: Mathematical and General* **31**,

- 4773 (1998).
- [41] D. Tapias and P. Sollich, Multifractality and statistical localization in highly heterogeneous random networks, *Europhysics Letters* **144**, 41001 (2023).
- [42] J. D. Silva and F. L. Metz, Analytic solution of the resolvent equations for heterogeneous random graphs: spectral and localization properties, *Journal of Physics: Complexity* **3**, 045012 (2022).
- [43] J. D. da Silva, D. Tapias, P. Sollich, and F. L. Metz, Spectral properties, localization transition and multifractal eigenvectors of the Laplacian on heterogeneous networks, *SciPost Phys.* **18**, 047 (2025).
- [44] A. Mirlin and Y. V. Fyodorov, Universality of level correlation function of sparse random matrices, *Journal of Physics A: Mathematical and General* **24**, 2273 (1991).
- [45] G. Biroli and R. Monasson, A single defect approximation for localized states on random lattices, *Journal of Physics A: Mathematical and General* **32**, L255 (1999).
- [46] G. Semerjian and L. F. Cugliandolo, Sparse random matrices: the eigenvalue spectrum revisited, *Journal of Physics A: Mathematical and General* **35**, 4837 (2002).
- [47] A. J. Martínez-Mendoza, A. Alcazar-López, and J. A. Méndez-Bermúdez, Scattering and transport properties of tight-binding random networks, *Phys. Rev. E* **88**, 012126 (2013).
- [48] J. Alt, R. Ducatez, and A. Knowles, Extremal eigenvalues of critical Erdős–Rényi graphs, *The Annals of Probability* **49**, 10.1214/20-AOP1483 (2021).
- [49] L. Erdős, A. Knowles, H.-T. Yau, and J. Yin, Spectral statistics of erdős–rényi graphs ii: Eigenvalue spacing and the extreme eigenvalues, *Communications in Mathematical Physics* **314**, 587 (2012).
- [50] L. Erdős, A. Knowles, H.-T. Yau, and J. Yin, Spectral statistics of Erdős–Rényi graphs I: Local semicircle law, *The Annals of Probability* **41**, 2279 (2013).
- [51] Y. He, A. Knowles, and M. Marozzi, Local law and complete eigenvector delocalization for supercritical Erdős–Rényi graphs, *The Annals of Probability* **47**, 3278 (2019).
- [52] K. Tikhomirov and P. Youssef, Outliers in spectrum of sparse wigner matrices, *Random Structures & Algorithms* **58**, 517 (2021), <https://onlinelibrary.wiley.com/doi/pdf/10.1002/rsa.20982>.
- [53] L. Haan and A. Ferreira, *Extreme value theory: an introduction*, Vol. 3 (Springer, 2006).
- [54] S. Kotz and S. Nadarajah, *Extreme value distributions: theory and applications* (world scientific, 2000).
- [55] Z. Zhao, M.-A. Filip, and A. J. Thom, Rapidly convergent quantum Monte Carlo using a Chebyshev projector, *Faraday Discussions* **254**, 429 (2024).
- [56] C. A. Tracy and H. Widom, Level-spacing distributions and the Airy kernel, *Communications in Mathematical Physics* **159**, 151 (1994).
- [57] C. A. Tracy and H. Widom, On orthogonal and symplectic matrix ensembles, *Commun. Math. Phys.* **177**, 727 (1996).
- [58] C. Nadal and S. N. Majumdar, A simple derivation of the Tracy-Widom distribution of the maximal eigenvalue of a Gaussian unitary random matrix, *Journal of Statistical Mechanics: Theory and Experiment* **2011**, P04001 (2011).
- [59] I. M. Johnstone and Z. Ma, Fast approach to the Tracy-Widom law at the edge of GOE and GUE, *The annals of applied probability: an official journal of the Institute of Mathematical Statistics* **22**, 1962 (2012).
- [60] Á. Nagy and E. Romera, Relative rényi entropy and fidelity susceptibility, *Europhysics Letters* **109**, 60002 (2015).
- [61] C. M. Soukoulis and E. N. Economou, Fractal character of eigenstates in disordered systems, *Phys. Rev. Lett.* **52**, 565 (1984).
- [62] A. Rodriguez, L. J. Vasquez, K. Slevin, and R. A. Römer, Critical parameters from a generalized multifractal analysis at the anderson transition, *Phys. Rev. Lett.* **105**, 046403 (2010).
- [63] F. Evers and A. D. Mirlin, Anderson transitions, *Rev. Mod. Phys.* **80**, 1355 (2008).
- [64] A. K. Das, A. Ghosh, and I. M. Khaymovich, Robust nonergodicity of the ground states in the β ensemble, *Phys. Rev. B* **109**, 064206 (2024).
- [65] A. K. Das, A. Ghosh, and I. M. Khaymovich, Emergent multifractality in power-law decaying eigenstates, *Phys. Rev. B* **112**, 024201 (2025).
- [66] D. J. Luitz, I. M. Khaymovich, and Y. B. Lev, Multifractality and its role in anomalous transport in the disordered XXZ spin-chain, *SciPost Phys. Core* **2**, 006 (2020).
- [67] A. Lakshminarayan, S. Tomsovic, O. Bohigas, and S. N. Majumdar, Extreme statistics of complex random and quantum chaotic states, *Phys. Rev. Lett.* **100**, 044103 (2008).
- [68] J. Lindinger, A. Buchleitner, and A. Rodríguez, Many-body multifractality throughout bosonic superfluid and Mott insulator phases, *Phys. Rev. Lett.* **122**, 106603 (2019).
- [69] S. Goldstein, J. L. Lebowitz, C. Mastrodonato, R. Tumulka, and N. Zanghì, Normal typicality and von neumann’s quantum ergodic theorem, *Proc. R. Soc. A: Math. Phys. Eng. Sci.* **466**, 3203 (2010).
- [70] A. Vikram and V. Galitski, Dynamical quantum ergodicity from energy level statistics, *Phys. Rev. Res.* **5**, 033126 (2023).
- [71] D. N. Page, Average entropy of a subsystem, *Phys. Rev. Lett.* **71**, 1291 (1993).
- [72] V. E. Kravtsov, I. M. Khaymovich, E. Cuevas, and M. Amini, A random matrix model with localization and ergodic transitions, *New J. Phys.* **17**, 122002 (2015).
- [73] A. De Luca, B. L. Altshuler, V. E. Kravtsov, and A. Scardicchio, Anderson localization on the bethe lattice: Nonergodicity of extended states, *Phys. Rev. Lett.* **113**, 046806 (2014).
- [74] A. K. Das and A. Ghosh, Nonergodic extended states in the β ensemble, *Phys. Rev. E* **105**, 054121 (2022).
- [75] N. Roy, J. Sutradhar, and S. Banerjee, Diagnostics of nonergodic extended states and many body localization proximity effect through real-space and fock-space excitations, *Physical Review B* **107**, 115155 (2023).
- [76] S. Popescu, A. J. Short, and A. Winter, Entanglement and the foundations of statistical mechanics, *Nat. Phys.* **2**, 754 (2006).
- [77] L. Amico, R. Fazio, A. Osterloh, and V. Vedral, Entanglement in many-body systems, *Rev. Mod. Phys.* **80**, 517 (2008).
- [78] S. Sinha and S. Sinha, Chaos and quantum scars in bose-josephson junction coupled to a bosonic mode, *Phys. Rev. Lett.* **125**, 134101 (2020).
- [79] G. De Tomasi and I. M. Khaymovich, Multifractality

- meets entanglement: Relation for nonergodic extended states, *Phys. Rev. Lett.* **124**, 200602 (2020).
- [80] M. Haque, P. A. McClarty, and I. M. Khaymovich, Entanglement of midspectrum eigenstates of chaotic many-body systems: Reasons for deviation from random ensembles, *Phys. Rev. E* **105**, 014109 (2022).
- [81] W. Buijsman, M. Haque, and I. M. Khaymovich, Power-law banded random matrix ensemble as a model for quantum many-body hamiltonians, *Phys. Rev. E* **113**, 034116 (2026).
- [82] E. N. Epperly, J. A. Tropp, and R. J. Webber, Xtrace: Making the most of every sample in stochastic trace estimation, *SIAM Journal on Matrix Analysis and Applications* **45**, 1 (2024), <https://doi.org/10.1137/23M1548323>.
- [83] L. Lin, Y. Saad, and C. Yang, Approximating spectral densities of large matrices, *SIAM Review* **58**, 34 (2016).
- [84] M. Pino, J. Tabanera, and P. Serna, From ergodic to non-ergodic chaos in Rosenzweig-Porter model, *J. Phys. A: Math. Theor.* **52**, 475101 (2019).
- [85] A. K. Das and A. Ghosh, Transport in deformed centrosymmetric networks, *Phys. Rev. E* **106**, 064112 (2022).
- [86] A. K. Das, Spectral statistics, nonequilibrium dynamics, and thermalization in random matrices with global F_2 -symmetry, *Phys. Rev. B*, (2026).
- [87] G. Livan, M. Novaes, and P. Vivo, The fluid semicircle, in *Introduction to Random Matrices: Theory and Practice* (Springer International Publishing, Cham, 2018) pp. 23–31.
- [88] R. Silver and H. Röder, Densities of states of mega-dimensional Hamiltonian matrices, *International Journal of Modern Physics C* **05**, 735 (1994).
- [89] L.-W. Wang, Calculating the density of states and optical-absorption spectra of large quantum systems by the plane-wave moments method, *Phys. Rev. B* **49**, 10154 (1994).
- [90] A. Weiße, G. Wellein, A. Alvermann, and H. Fehske, The kernel polynomial method, *Rev. Mod. Phys.* **78**, 275 (2006).
- [91] R. Haydock, V. Heine, and M. Kelly, Electronic structure based on the local atomic environment for tight-binding bands. ii, *Journal of Physics C: Solid State Physics* **8**, 2591 (1975).
- [92] P. Akara-pipattana and O. Evnin, Hammerstein equations for sparse random matrices, *Journal of Physics A: Mathematical and Theoretical* **58**, 035006 (2025).
- [93] A. C. Bertuola, J. X. de Carvalho, M. S. Hussein, M. P. Pato, and A. J. Sargeant, Level density for deformations of the Gaussian orthogonal ensemble, *Phys. Rev. E* **71**, 036117 (2005).
- [94] A. K. Das, A. Ghosh, and L. F. Santos, Spectral form factor and energy correlations in banded random matrices, *Phys. Rev. B* **111**, 224202 (2025).
- [95] B. Roy, A. K. Das, A. Ghosh, and I. M. Khaymovich, Anomalous energy correlations and spectral form factor in the nonergodic phase of the β -ensemble, *Phys. Rev. B* (2025).
- [96] O. Bohigas, M. J. Giannoni, and C. Schmit, Characterization of chaotic quantum spectra and universality of level fluctuation laws, *Phys. Rev. Lett.* **52**, 1 (1984).
- [97] M. Berry and M. Tabor, Level clustering in the regular spectrum, *Proc. R. Soc. Lond. A* **356**, 375 (1977).
- [98] M. Mehta, *Random Matrices*, Pure and Applied Mathematics (Elsevier Science, 2004).
- [99] T. Guhr, A. Müller–Groeling, and H. A. Weidenmüller, Random-matrix theories in quantum physics: common concepts, *Phys. Rep.* **299**, 189 (1998).
- [100] B. Dietz and F. Haake, Taylor and Padé analysis of the level spacing distributions of random-matrix ensembles, *Zeitschrift für Physik B Condensed Matter* **80**, 153 (1990).
- [101] A. K. Das and A. Ghosh, Eigenvalue statistics for generalized symmetric and hermitian matrices, *J. Phys. A: Math. Theor.* **52**, 395001 (2019).
- [102] A. K. Das and A. Ghosh, Dynamical signatures of chaos to integrability crossover in 2×2 generalized random matrix ensembles, *J. Phys. A: Mathematical and Theoretical* 10.1088/1751-8121/ad0b5a (2023).
- [103] A. Jackson, C. Mejia-Monasterio, T. Rupp, M. Saltzer, and T. Wilke, Spectral ergodicity and normal modes in ensembles of sparse matrices, *Nuclear Physics A* **687**, 405 (2001).
- [104] J. M. G. Gómez, R. A. Molina, A. Relaño, and J. Retamosa, Misleading signatures of quantum chaos, *Phys. Rev. E* **66**, 036209 (2002).
- [105] V. Oganesyan and D. A. Huse, Localization of interacting fermions at high temperature, *Phys. Rev. B* **75**, 155111 (2007).
- [106] Y. Y. Atas, E. Bogomolny, O. Giraud, and G. Roux, Distribution of the ratio of consecutive level spacings in random matrix ensembles, *Phys. Rev. Lett.* **110**, 084101 (2013).
- [107] A. K. Das, A. Ghosh, and I. M. Khaymovich, Absence of mobility edge in short-range uncorrelated disordered model: Coexistence of localized and extended states, *Phys. Rev. Lett.* **131**, 166401 (2023).
- [108] F. J. Dyson, Statistical theory of the energy levels of complex systems. i, *Journal of Mathematical Physics* **3**, 140 (1962).
- [109] F. J. Dyson, A brownian-motion model for the eigenvalues of a random matrix, *Journal of Mathematical Physics* **3**, 1191 (1962).
- [110] A. Pandey and R. Ramaswamy, Level spacings for harmonic-oscillator systems, *Phys. Rev. A* **43**, 4237 (1991).
- [111] S. Sorathia, F. M. Izrailev, V. G. Zelevinsky, and G. L. Celardo, From closed to open one-dimensional anderson model: Transport versus spectral statistics, *Phys. Rev. E* **86**, 011142 (2012).
- [112] E. J. Torres-Herrera, J. A. Méndez-Bermúdez, and L. F. Santos, Level repulsion and dynamics in the finite one-dimensional anderson model, *Phys. Rev. E* **100**, 022142 (2019).
- [113] A. Andersen, A. Jackson, and H. Pedersen, Rigidity and normal modes in random matrix spectra, *Nuclear Physics A* **650**, 213 (1999).
- [114] A. Bäcker, F. Steiner, and P. Stifter, Spectral statistics in the quantized cardioid billiard, *Phys. Rev. E* **52**, 2463 (1995).
- [115] K. Efetov, Supersymmetry and theory of disordered metals, *advances in Physics* **32**, 53 (1983).
- [116] E. Cuevas, E. Louis, M. Ortuño, and J. A. Vergés, Energy fluctuations, Thouless energy, and conductance in the Anderson model in the ballistic and diffusive regimes, *Phys. Rev. B* **56**, 15853 (1997).
- [117] P. Sierant, D. Delande, and J. Zakrzewski, Thouless time analysis of Anderson and many-body localization

- transitions, *Phys. Rev. Lett.* **124**, 186601 (2020).
- [118] C. L. Bertrand and A. M. García-García, Anomalous Thouless energy and critical statistics on the metallic side of the many-body localization transition, *Phys. Rev. B* **94**, 144201 (2016).
- [119] M. Serbyn, Z. Papić, and D. A. Abanin, Thouless energy and multifractality across the many-body localization transition, *Phys. Rev. B* **96**, 104201 (2017).
- [120] A. M. García-García, Y. Jia, and J. J. M. Verbaarschot, Universality and Thouless energy in the supersymmetric Sachdev-Ye-Kitaev model, *Phys. Rev. D* **97**, 106003 (2018).
- [121] M. Schiulaz, E. J. Torres-Herrera, and L. F. Santos, Thouless and relaxation time scales in many-body quantum systems, *Phys. Rev. B* **99**, 174313 (2019).
- [122] A. L. Corps, R. A. Molina, and A. Relaño, Thouless energy challenges thermalization on the ergodic side of the many-body localization transition, *Phys. Rev. B* **102**, 014201 (2020).
- [123] A. K. Das and A. Ghosh, Chaos due to symmetry-breaking in deformed poisson ensemble, *JSTAT* **2022** (6), 063101.
- [124] L. Erdős and A. Knowles, The Altshuler–Shklovskii formulas for random band matrices I: the unimodular case, *Commun. Math. Phys.* **333**, 1365 (2015).
- [125] D. J. Thouless, Electrons in disordered systems and the theory of localization, *Physics Reports* **13**, 93 (1974).
- [126] D. Thouless, Phase transitions for the one-dimensional landau-ginzburg system and their relation to the theory of polymers and of electrons in a random potential, *Journal of Physics C: Solid State Physics* **8**, 1803 (1975).
- [127] D. J. Thouless, Maximum metallic resistance in thin wires, *Phys. Rev. Lett.* **39**, 1167 (1977).
- [128] U. Sivan and Y. Imry, Energy-level correlation function and ac conductivity of a finite disordered system, *Phys. Rev. B* **35**, 6074 (1987).
- [129] A. G. Aronov and A. D. Mirlin, Fluctuations of the number of energy levels at the mobility edge, *Phys. Rev. B* **51**, 6131 (1995).
- [130] A. Jagannathan and M. Tarzia, Electronic states of a disordered two-dimensional quasiperiodic tiling: From critical states to Anderson localization, *Phys. Rev. B* **107**, 054206 (2023).
- [131] E. Faleiro, J. M. G. Gómez, R. A. Molina, L. Muñoz, A. Relaño, and J. Retamosa, Theoretical derivation of $1/f$ noise in quantum chaos, *Phys. Rev. Lett.* **93**, 244101 (2004).
- [132] R. Riser, V. A. Osipov, and E. Kanzieper, Power spectrum of long eigenlevel sequences in quantum chaotic systems, *Phys. Rev. Lett.* **118**, 204101 (2017).
- [133] A. L. Corps and A. Relaño, Long-range level correlations in quantum systems with finite Hilbert space dimension, *Phys. Rev. E* **103**, 012208 (2021).
- [134] R. Berkovits, Super-Poissonian behavior of the Rosenzweig-Porter model in the nonergodic extended regime, *Phys. Rev. B* **102**, 165140 (2020).
- [135] E. Granet, Y. Kikuchi, H. Dreyer, and E. Rinaldi, Simulating sparse syk model with a randomized algorithm on a trapped-ion quantum computer, *npj Quantum Information* (2026).
- [136] M. Bauer and O. Golinelli, Random incidence matrices: moments of the spectral density, *Journal of Statistical Physics* **103**, 301 (2001).